Sakarya Üniversitesi Fen Bilimleri Dergisi
Sakarya University Journal of Science

e-ISSN : 2147-835X
Publisher : Sakarya University

Vol. 30, No. 4, 562-579, 2026
DOI: https://doi.org/10.16984/saufenbilder.1786927

Research Article

Chalcone-Appended Metallophthalocyanines: Synthesis, Redox Properties, and Catalytic Oxidation of 2-Mercaptoethanol

Hüseyin Karaca[1*], Özlem Güven[1,2], M. Dinesh Kumar[3], Raju Ravikumar[3]

[1]Department of Chemistry, Science Faculty, Sakarya University, 54050 Sakarya, Türkiye, karaca@sakarya.edu.tr
[2]Ferrero Fındık, Yaylacık, Kanalyolu Cd No:14, 41140 Başiskele, Kocaeli, Türkiye, ozlem.senturk1@ogr.sakarya.edu.tr
[3]Department of Chemistry, Dr. N.G.P. Arts and Science College, Coimbatore- 641048, (Tamil Nadu) India, dineshkumarm@drngpasc.ac.in, ravikumar.r@drngpasc.ac.in

[*]Corresponding Authors

ARTICLE INFO

Keywords:
Chalcone
Phthalocyanine
Redox
Characterization
Spectroelectrochemistry
Catalysis

Article History:
Received: 19.09.2025
Revised: 14.04.2026
Accepted: 16.05.2026
Online Available: 23.07.2026

ABSTRACT

A novel series of metallophthalocyanines (M = Zn, Co, Cd), each bearing four peripheral chalcone groups, was synthesized and its characterization was carried out through FT-IR, NMR (^{1}H and ^{13}C), HRMS, UV-Vis spectroscopy. Electrochemical investigations revealed distinctive redox behaviors for each complex. Notably, Pc-6 underwent non-reversible reduction (−0.86 V) and oxidation (0.20 V), while Pc-7 and Pc-8 showed reversible reductions at −0.65 V and −0.64 V, respectively. Spectroelectrochemical analysis indicated that Pc-6 and Pc-8 rapidly decomposed following ring-based redox events, whereas Pc-7 displayed a more stable and dynamic transformation, characterized by distinct isosbestic points and the emergence of new absorption bands. This behavior underscores the enhanced electronic delocalization and redox stability of Pc-7. Furthermore, Pc-7 demonstrated catalytic activity in the oxidation of 2-mercaptoethanol, yielding a turnover number of 45.84 and an initial rate of 0.084 μmol·s^{-1}. These results highlight the potential of chalcone-functionalized phthalocyanines, especially Pc-7, as robust redox-active and catalytic materials.

1. Introduction

Phthalocyanines, both metal-free and metallo variants, have been known for a century and are among the most extensively researched macrocyclic molecules. They share this distinction with biologically occurring porphyrins [1-8]. These compounds have garnered significant attention due to their valuable characteristics, including optical, electronic, electrical, photoelectric, and electrochemical properties [9-23]. Consequently, they have become the primary focus of research in the development of innovative electronic devices, gas sensors, detectors, catalytic reactions, and solar cells [24-36].

However, strong intermolecular interactions resulting from intramolecular π-π interactions among phthalocyanines lead to aggregation, which adversely impacts their solubility. This limitation hinders the full exploitation of their exceptional properties. To overcome this challenge, researchers have explored various approaches, such as attaching different functional groups or designing new molecules to bind to phthalocyanines, either at their periphery or non-peripheral positions [37-39]. Each of these attached groups or molecules imparts distinctive properties to phthalocyanines, further expanding their potential applications.

Chalcones, aromatic ketones and enones, serve as the fundamental building blocks for numerous biologically active compounds, boasting valuable properties including anti-cancer [40, 41], antioxidant [42-44], antimicrobial [45-49], cytotoxic [50-53], analgesic [54-58], and antipyretic [59, 60] effects. Moreover, they are recognized as precursors in the synthesis of

Cite as: H. Karaca, Ö. Güven, M.D. Kumar, R. Ravikumar "Chalcone-appended metallophthalocyanines: Synthesis, redox properties, and catalytic oxidation of 2-mercaptoethanol" *Sakarya University Journal of Science,* vol. 30, no. 4, pp. 562-579, 2026. https://doi.org/10.16984/saufenbilder.1786927

This is an open access paper distributed under the terms and conditions of the Creative Commons Attribution-NonCommercial 4.0 International License.

flavonoids and isoflavonoids [61, 62]. The creation of a basic chalcone compound typically involves aldol condensation, achieved through a sodium hydroxide-catalyzed reaction between an aldehyde and a ketone [63-66]. Chalcones possess excellent solubility and their inherent biological activities make them readily applicable in biological systems. Furthermore, they have been explored for a wide range of applications, including electrocatalysis [67, 68], photodynamic therapy [69], enzyme inhibition [70, 71], photodiode properties, photophysical and photochemical characteristics, metal sensing applications [72], DNA-binding, enzyme inhibition [73], as well as the synthesis, spectral analysis, electrochemical properties, and spectroelectrochemical properties of metallophthalocyanines substituted with chalcone moieties. These areas have become the focus of both experimental and theoretical investigations.

In this research, we will explore the synthesis of a phthalocyanine compound derived from chalcone and examine its electrochemical and spectroelectrochemical properties. We aim to compare the experimental spectroscopic findings with data calculated using the Density Functional Theory (DFT) method. The starting material for this endeavor is (E)-4-(4-(3-(4-methoxyphenyl)-3-oxoprop-1-en-1-yl)phenoxy)phthalonitrile, referred to as compound 5.

The newly designed metallophthalocyanines with chalcone substituents on the periphery were subjected to characterization through various analytical techniques, including ^{1}H-NMR, ^{13}C-NMR, IR, MALDI-TOF, and UV/Vis spectra. Additionally, we reported the theoretically calculated spectral data obtained through the DFT/B3LYP method.

2. Experimental

2.1. General

The glass materials were first heated to 150°C for an hour, then cooled in dessicator before the experiments. High-quality chemicals were commercially sourced and used without further purification. A Barnstead Electrothermal 9200 device was employed for melting purposes. A thick-walled glass column was packed with Merck Silica Gel 60 for performing flash column chromatography. To monitor the reactions via chromatography, Merck Silica Gel PF-254 was utilized. Phosphomolybdic acid solution in ethanol, along with UV light, was used to reveal the spots on the chromatography. Anhydrous magnesium sulfate served as the drying agent for the solvents, while the solvent was evaporated by means of a rotary evaporator.

2.2. Spectroscopic Analysis

The ^{1}H and ^{13}C NMR spectra were measured on 300 MHz VARIAN Infinity Plus NMR spectrometer. The chemical shifts were recorded in ppm relative to CDCl3 (δ 7.26 for 1H and δ 77.0 for 13C), and DMSO-d6 as internal standards. FT-IR spectra were recorded on a Perkin Elmer Spectrum Two. HRMS and MALDI-TOF mass spectra were recorded with a Bruker Daltonics flexAnalysis system. UV-Visible spectroscopy was recorded on a Shimadzu UV 2600 Spectrophotometer.

2.3. Catalytic Oxidation of 2-Mercaptoethanol

To ensure the reproducibility of the catalytic results, all oxidation experiments were conducted under strictly controlled conditions, with the temperature maintained at 25°C and the pH of the reaction medium kept constant throughout the study. The catalytic oxidation reaction was continuously monitored using an oxygen meter (CyberScan DO 300) within a closed system. In this setup, Co(II)phthalocyanine (Co(II)Pc) was dissolved in 200 mL of THF, resulting in a total of 3.16 µmol of the compound. The reaction mixture was oxygen-saturated by bubbling air through it, with atmospheric oxygen serving as the oxidizing agent.

The catalytic reaction was initiated by introducing 2.07 mmol of 2-mercaptoethanol into the solution. The ratio of 2-mercaptoethanol to Co(II) phthalocyanine was maintained at 654:1, which was found to be an effective catalytic activity ratio. 1 mL of a 0.25 wt% aqueous sodium hydroxide solution was introduced to the reactor, along with 2-mercaptoethanol, to facilitate the reaction. The

dissolved oxygen remaining in the mixture was continuously monitored, allowing for the calculation of time-dependent oxygen consumption. Various parameters were computed to characterize the catalytic activity of Co(II)phthalocyanine, including the turnover number (TON), the initial rate of reaction (µmol $O_2.s^{-1}$), and the overall consumption rate of oxygen (µmol.min^{-1}). To derive the turnover number, the moles of oxygen were divided by the moles of phthalocyanine, with the initial reaction rate being calculated by setting the first derivative of the rate equation to zero. The oxygen consumption rate was computed by dividing the moles of oxygen consumed by the respective time period [33, 38, 74-76].

2.4. Synthesis

2.4.1. Synthesis of (E)-3-(4-hydroxyphenyl)-1-(4-methoxyphenyl)prop-2-en-1-one, 3

To prepare compound 3, a solution of KOH (9.20 g) in a mixture of water and ethanol (1:1, 60 mL) was prepared. 4-hidroksibenzaldehit, **1**, (41 mmol, 5.00 g) was added into this solution by stirring. Then 4-methoxyacetophenone, **2,** (41 mmol, 1.23 g) was introduced into the same solution. The reaction mixture was kept stirring at room temperature under nitrogen for 24 hours. Afterward, it was transferred to a beaker, and an aqueous HCl solution was added to neutralize the basic medium. The solid precipitate formed was filtered using a sintered funnel and recrystallized in ethanol. This yielded a light yellow solid with a melting point of 193-195 °C and a chemical yield of 2.95 g (28.4%). The compound was characterized by FT-IR (ATR System, cm^{-1}), showing peaks at 3146, 3025, 2933, 2836, 1629, 1582, 1566, 1555, 1504, 1367, 1339, 1318, 1272, 1207, 1174, 1160, 1102, 1031, 1012, 1002, 988, 970, 938, 873, 882, 812, and 777. Additionally, the ^{1}H NMR (300 MHz, DMSO-d6) spectrum displayed signals at δ 10.07 (s, 1H), 8.06 (d, J = 7.24, 2H), 7.73–7.48 (m, 5H), 7.45–7.34 (m, 1H), 6.79 (d, J = 8.40, 2H), and 3.75 (s, 3H). The ^{13}C NMR (75 MHz, DMSO-d6) spectrum exhibited signals at δ 189.1, 160.2, 144.6, 138.1, 131.2 (2C), 128.7 (2C), 128.4 (2C), 125.8 (2C), 118.8, 116.1 (2C), and 55.2. The exact mass was determined to be 254.09, and the HRMS data showed a calculated m/z value for C16H14O3 as 254.29, with a found value of $[M + 2H]^+$ at 256.04.

2.4.2. Synthesis of Target Phthalonitrile, 5

In a round-bottom flask, compound 3 (9.83 mmol, 2.50 g) and 4-nitrophthalonitrile (9.83 mmol, 1.70 g) were dissolved together in 40 mL of DMSO and stirred under a nitrogen atmosphere. After the addition of potassium carbonate (2.72 g, 19.66 mmol), the reaction was allowed to continue stirring for 24 hours. The reaction was quenched by reaction mixture into 50 mL of water. Extraction was performed using a mixture of dichloromethane and water. Anhydrous magnesium sulfate ($MgSO_4$) was used to dry the organic layer, and the remaining solvent in the mixture was evaporated under vacuum. The resulting yellow solid obtained from this process was filtered and subjected to recrystallization in ethanol. The compound had a melting point of 177-179 °C, and the chemical yield was 1.95 g (52.1%). For the compound's characterization, FT-IR (ATR System, cm^{-1}) was applied, The peaks are at 3060, 3042, 2936, 2924, 2838, 2231, 1651, 1605, 1581, 1556, 1502, 1479, 1439, 1401, 1331, 1280, 1249, 1206, 1169, 1152, 1104, 1088, 1038, 1012, 963, 944, 892, 869, 850, 834, and 822 cm^{-1}. The ^{1}H NMR (300 MHz, DMSO-d6) spectrum displayed signals at δ 8.16-8.10 (m, 3H), 8.01 (d, J = 6.97, 1H), 7.88 (s, 1H), 7.54–7.52 (m, 4H), 7.06-6.95 (m, 4H), and 3.69 (s, 3H). The ^{13}C NMR (75 MHz, DMSO-d6) spectrum exhibited signals at δ 189.6, 160.5, 154.8, 142.5, 137.5, 135.1, 132.6, 132.5, 130.7 (2C), 128.2 (2C), 128.1 (2C), 122.4, 122.2, 121.4 (2C), 120.4, 117.3, 115.1, 114.9, and 109.1, with a ^{13}C signal at 55.1. The exact mass was found to be 380.12, and HRMS data showed a calculated m/z value for $C_{24}H_{16}N_2O_3$ as 380.40, with a found value of $[M+2H]^+$ at 382.29.

2.4.3. Synthesis of Zinc Phthalocyanine, Pc-6

To synthesize ZnPc, **5** (0.50 g, 1.31 mmol) was dissolved in a mixture of DMEA and DMF (1:2). Zinc acetate dihydrate (73.5 mg, 0.33 mmol) was added, and then stirred at 160 °C by refluxing under nitrogen atmosphere for 24 hours. The reaction was quenched into a mixture of methanol and water (1:1). The precipitate was filtered and washed. The dark green solid was

then dissolved in dichloromethane, dried with $MgSO_4$, and evaporated. The residue was purified by column chromatography on silica gel, using a mixture of ethyl acetate/hexane (1:5). This purification process yielded a dark green solid with a melting point greater than 300 °C and a chemical yield of 0.214 g (41.0%). The compound was characterized by FT-IR (ATR System, cm^{-1}), showing peaks at 3176, 3040, 2938, 2912, 2838, 1762, 1726, 1642, 1576, 1564, 1466, 1445, 1414, 1385, 1348, 1329, 1246, 1218, 1203, 1145, 1057, 1022, 1008, 978, 943, 921, 882, 825, and 776. The ^1H NMR (300 MHz, DMSO-d6) spectrum displayed signals at δ 8.04–7.98 (m, 5H), 7.88–7.78 (m, 5H), 7.73–7.68 (m, 10H), 7.61–7.55 (m, 5H), 7.53–7.49 (m, 15H), 7.38–7.33 (m, 8H), 7.14–7.09 (m, 4H), and 3.86-3.70 (m, 12H). MALDI-TOF MS data showed a calculated m/z value for $C_{96}H_{64}N_8O_{12}Zn$ as 1586.99, with a found value of $[M + 2H]^+$ at 1588.8.

2.4.4. Synthesis of Cobalt(II) Phthalocyanine, Pc-7

For the synthesis of **Pc-7**, compound **5** (0.50 g, 1.31 mmol) was dissolved in a mixture of DMEA and DMF (1:2). Cobalt(II) acetate tetrahydrate (81.4 mg, 0.33 mmol) was added to the mixture, and the stirred at 160 °C under reflux in a nitrogen atmosphere for 24 hours. The reaction was quenched into a mixture of methanol and water (1:1). The precipitate was filtered and washed with methanol. The dark green solid was dissolved in dichloromethane and dried with $MgSO_4$, and then the solvent was evaporated. The residue was purified by column chromatography on silica gel, using a mixture of ethyl acetate/hexane (1:5). The purification process yielded a dark green solid with a melting point greater than 300 °C and a chemical yield of 0.223 g (43.0%). Characterization of the compound was carried out by FT-IR (ATR System, cm^{-1}), revealing peaks at 3064, 3037, 2918, 2845, 1706, 1648, 1580, 1562, 1518, 1508, 1461, 1439, 1404, 1327, 1256, 1227, 1211, 1164, 1112, 1089, 1052, 1029, 1015, 978, 950, 871, and 773. MALDI-TOF MS data showed a calculated m/z value for $C_{96}H_{64}N_8O_{12}Co$ as 1580.55, with a found value of $[M + 2H]^+$ at 1582.4.

2.4.5. Synthesis of Cadmium(II) Phthalocyanine, Pc-8

For the synthesis of Cadmium(II) Phthalocyanine, compound **5** (0.50 g, 1.31 mmol) was dissolved in a mixture of DMEA and DMF (1:2). Cadmium acetate dihydrate (87 mg, 0.33 mmol) was added, and stirred at 160 °C under reflux in a nitrogen atmosphere for 24 hours [77]. The reaction was quenched into a mixture of methanol and water (1:1). The precipitate was filtered and washed with methanol. The dark green solid was then dissolved in dichloromethane, dried with $MgSO_4$, and the solvent was evaporated. The residue was further purified by column chromatography on silica gel, with an ethyl acetate/hexane mixture (1:5). The purification process yielded a dark green solid with a melting point greater than 300 °C and a chemical yield of 0.126 g (23.5%). Characterization of the compound was carried out by FT-IR (ATR System, cm^{-1}), revealing peaks at 3068, 2928, 1721, 1654, 1566, 1551, 1452, 1435, 1402, 1368, 1327, 1299, 1254, 1205, 1130, 1071, 1042, 1018, 987, 954, 936, 878, 854, and 775. The ^1H NMR (300 MHz, DMSO-d6) spectrum displayed signals at δ 8.11–7.72 (m, 20H), 7.65–7.44 (m, 20H), 7.36–7.03 (m, 12H), and 3.82-3.64 (m, 12H). MALDI-TOF MS data showed a calculated m/z value for $C_{96}H_{64}N_8O_{12}Cd$ as 1634.02, with a found value of $[M + 2H]^+$ at 1635.9.

2.5. Quantum Chemical Calculations

Quantum chemical calculations were employed to determine various electronic properties, including HOMO (Highest Occupied Molecular Orbital), LUMO (Lowest Unoccupied Molecular Orbital), ΔE (Energy Gap), chemical hardness, global softness, electronegativity, nucleophilicity, and chemical potential. These calculations were carried out using Gaussian 16W [78], and the results were visualized using GausView 6.0.16 [79]. For calculating the quantum chemical properties of the monomer phthalonitrile **5**, the Hartree-Fock and B3LYP [80] methods, coupled with the 6-311++G(d,p) basis set, were applied.

3. Results and Discussion

3.1. Synthesis

To initiate the synthesis of the target Phthalocyanines (Pcs), the first step involved the synthesis of chalcone derivative **(Compound 3)**. This was achieved by reacting **4-hydroxybenzaldehyde (Compound 1)** and 4-methoxyacetophenone in a mixture of ethanol and water, with the assistance of KOH as a catalyst. After purification using flash column chromatography, the reaction yielded a light yellow solid with a calculated yield of 28.4%. **This relatively low yield is attributed to the rigorous purification steps and multiple washing processes carried out to ensure high chemical purity for the subsequent stages.** This synthesized chalcone **compound 3** was then used as a starting material to synthesize a new chalcone-derived phthalonitrile compound, known as **compound 5**, through an SNAr (Nucleophilic Aromatic Substitution) reaction between **compound 3** and 4-nitrophthalonitrile (Scheme 1).

After the synthesis of compound 5, flash column chromatography was employed, resulting in a chemical reaction yield of 52.1% for phthalonitrile 5. The structures of compounds **3** and **5** were determined using ^{1}H and ^{13}C NMR spectra. Furthermore, the synthesized molecules, compounds 3 and 5, were confirmed through FT-IR spectra. Compound 5, the phthalonitrile, served as the starting material for the production of metallophthalocyanines (MPcs). Zinc acetate dihydrate ($Zn(OAc)_2 \cdot 2H_2O$), cobalt acetate tetrahydrate ($Co(OAc)_2 \cdot 4H_2O$), and cadmium acetate dihydrate were used as the metal ion sources to create the central metal ions in the phthalocyanines: Zn^{2+}, Co^{2+}, and Cd^{2+}. As anticipated, the cyclotetramerization reaction produced an isomeric mixture of the desired MPcs (as shown in Scheme 2).

For various applications such as catalysis, metal sensing, or electrochemistry, the solubility of the Phthalocyanines (Pcs) is of great importance [33, 37, 38, 81-84]. Solubility in the solvent affects the interaction of the Pcs with other species. **Pc-6** exhibited excellent solubility in dichloromethane and chloroform, so its NMR spectra were obtained in $CDCl_3$.

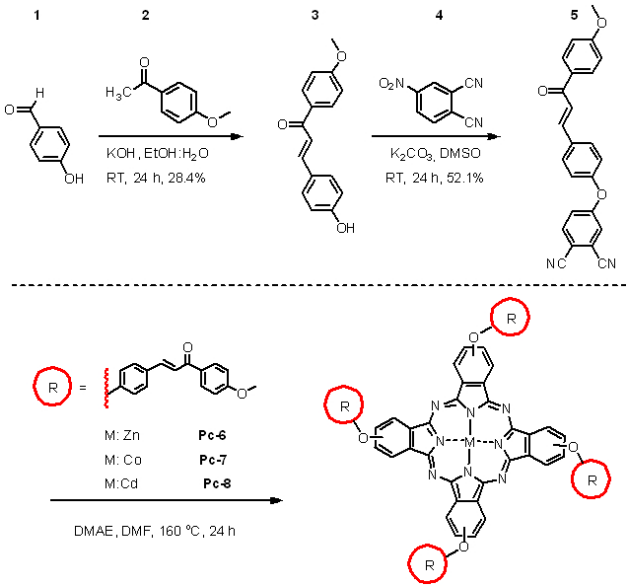

Scheme 1. Synthesis of target phthalonitrile **5** and the target Phthalocyanines (Pcs)

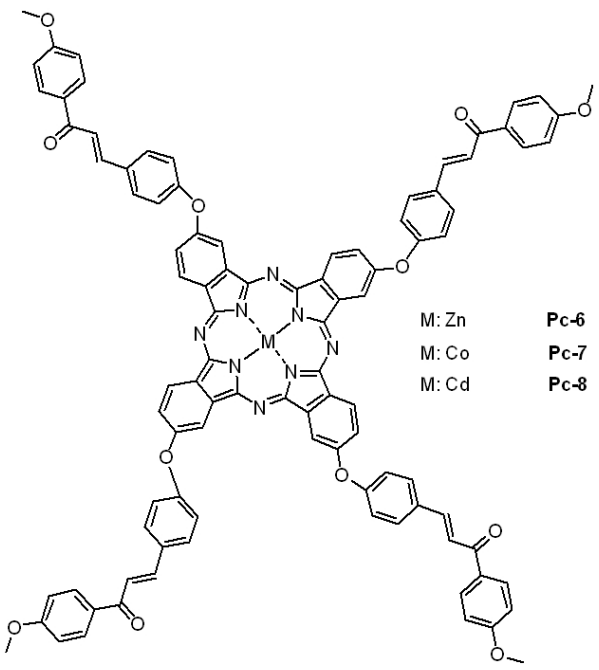

Scheme 2. The target phthalocyanines

The ^{1}H NMR spectrum of the Co(II)Pc (Pc-7) could not be recorded due to the **paramagnetic nature** of the cobalt central metal, which causes excessive line broadening and prevents meaningful signal resolution. Additionally, the observed broad multiplets in the ^{1}H NMR spectra of the other synthesized phthalocyanines are attributed to **molecular aggregation effects** arising from π-π interactions between the macrocyclic rings, even in diluted solutions.

Regarding the FT-IR analysis, the slight shifts in C=O stretching vibrations indicate changes in the **electronic environment and conjugation** within the chalcone substituents upon their peripheral attachment to the phthalocyanine core. **Pc-7** and **Pc-8** were highly soluble in dichloromethane but only slightly soluble in chloroform. All of these phthalocyanines exhibited good solubility in DMSO. The structures of the novel Pc compounds were characterized using instrumental analytic techniques.

3.2. Structure Elucidation

FT-IR spectra were obtained to confirm the structures of the compounds at different stages of the reaction. In the FT-IR spectra, various characteristic bands shifted as the reaction progressed. For instance, the band at 1651 cm^{-1}, indicative of the stretching vibration of C=O carbonyl bonds in compound 5, shifted to 1726 cm^{-1} for **Pc-6**, 1706 cm^{-1} for **Pc-7**, and 1721 cm^{-1} for **Pc-8** in the phthalocyanines. Similarly, the band at 1605 cm^{-1}, because of the stretching movement of C=C bonds in the molecule **5**, **shifted to 1642 cm^{-1} for Pc-6, 1648 cm^{-1} for Pc-7, and 1654 cm^{-1} for Pc-8 in the phthalocyanines. During the synthesis of compound 5, the phenolic OH band at 3146 cm^{-1} disappeared, and a strong characteristic band for CN triple bond vibration at 2231 cm^{-1} appeared.**

This CN vibration band disappeared after the synthesis of the phthalocyanines, serving as evidence of the cyclotetramerization of monomer **5** in the FT-IR spectrum of all MPcs.

Disappearance of the CN vibration band post-synthesis demonstrates the cyclotetramerization of monomer 5, as evidenced by the FT-IR spectra of the resulting MPcs. Other bands below 2000 cm^{-1} did not exhibit characteristic changes. The absorption bands at 3176, 3040, 2938, 2912, 2838, 1762, 1726, 1642, 1576, 1564, 1466, 1445, 1414, 1385, 1348, 1329, 1246, 1218, 1203, 1145, 1057, 1022, 1008, 978, 943, 921, 882, 825, and 776 cm^{-1} were observed for **Pc-6**, and these bands are associated with the skeletal vibrations of phthalocyanine [39, 85]. **Pc-7** exhibited very similar bands between 3064 and 773 cm^{-1}, while **Pc-8** showed bands between 3068 and 775 cm^{-1} in their FT-IR spectra.

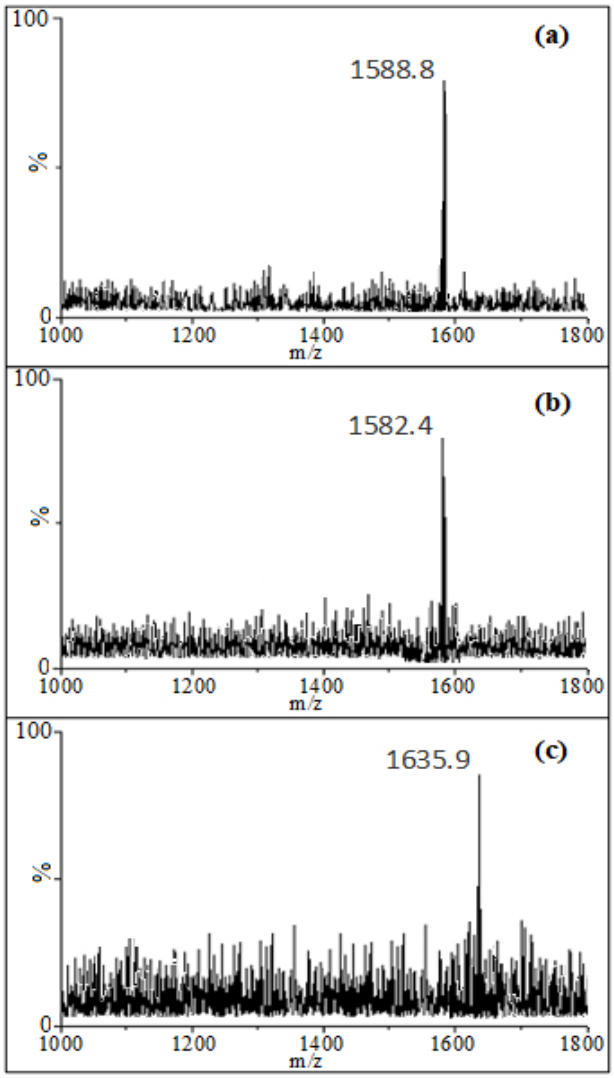

Figure 1. MALDI-TOF MS data of (a) ZnPc, (b) Co(II)Pc and (c) Cd(II)Pc

In the ^{1}H NMR spectra of compounds **3** and **5**, peaks were observed between 7 and 8.16 ppm due to the characteristic aromatic structure. Compound **3** displayed a peak at 10.07 ppm attributed to OH, which disappeared upon the synthesis of compound **5**. Additionally, the band at 3.75 ppm in compound **3**, attributed to methyl, continued to exist at 3.69 ppm in compound **5**. These changes indicated the success of these syntheses. When compound **5** underwent cyclotetramerization, the fused benzene rings in the resulting phthalocyanine structure produced distinct proton signals in the upfield region, similar to the proton signals of the phthalonitrile precursors. The 1H-NMR spectra of the target phthalocyanines revealed peaks with subtle chemical shift changes. Figure 1 shows the

MALDI-TOF MS spectra of metallophthalocyanines.

The presence of the molecular ion peaks at m/z = 1588.8 $[M+2H]^+$, 1582.4 [M+2H]+, and 1635.9 [M+2H]+ for ZnPc, Co(II)Pc and Cd(II)Pc, verifies the successful synthesis of the intended phthalocyanines.

3.3. Electrochemical and Spectroelectro-Chemical Measurements

Cyclic voltammograms were recorded using a Parstat potentiostat. In the three-electrode configuration, a Glassy Carbon Electrode (GCE) served as the working electrode, a Pt wire as the counter electrode, and Ag/AgCl as the reference electrode. Dimethylsulfoxide (DMSO) of extra-pure quality was used as the solvent, and a 0.1 mol/L solution of tetra-n-butylammonium tetrafluoroborate ($TBABF_4$, 99%) served as the supporting electrolyte.

Figure 2 illustrates the cyclic voltammograms for the metallophthalocyanines in the DMSO/$TBABF_4$ solution. In Figure 2, (a) shows non-reversible reduction at -0.86 V and non-reversible oxidation at 0.20 V for **Pc-6**. Figure 2 (b) displays a reversible reduction pair at -0.65 V for **Pc-7**. In the cyclic voltammetric study of **Pc-8**, as shown in Figure 2 (c), a reversible reduction at -0.64 V can be observed.

Spectroelectrochemical studies were conducted using an Optically Transparent Thin-Layer Electrode (OTTLE) cell kit, as depicted in Figure 3 and Figure 4.

For ZnPc, a prominent Q band was detected at 679 nm in DMSO, with a shoulder at 648 nm and a vibronic band at 610 nm, as well as a Soret band peaking at 394 nm (Figure 3 **(a)** and **(b)**). Similarly, Co(II)Pcexhibited a strong Q band at 662 nm in DMSO, with a shoulder at 648 nm, a vibronic band at 602 nm, and a Soret band at 394 nm (Figure 4 **(a)**). Cd(II)Pc showed a strong Q band at 684 nm in DMSO, with a shoulder at 655 nm, a vibronic band at 614 nm, and a Soret band at 394 nm (Figure 4 **(b)**).

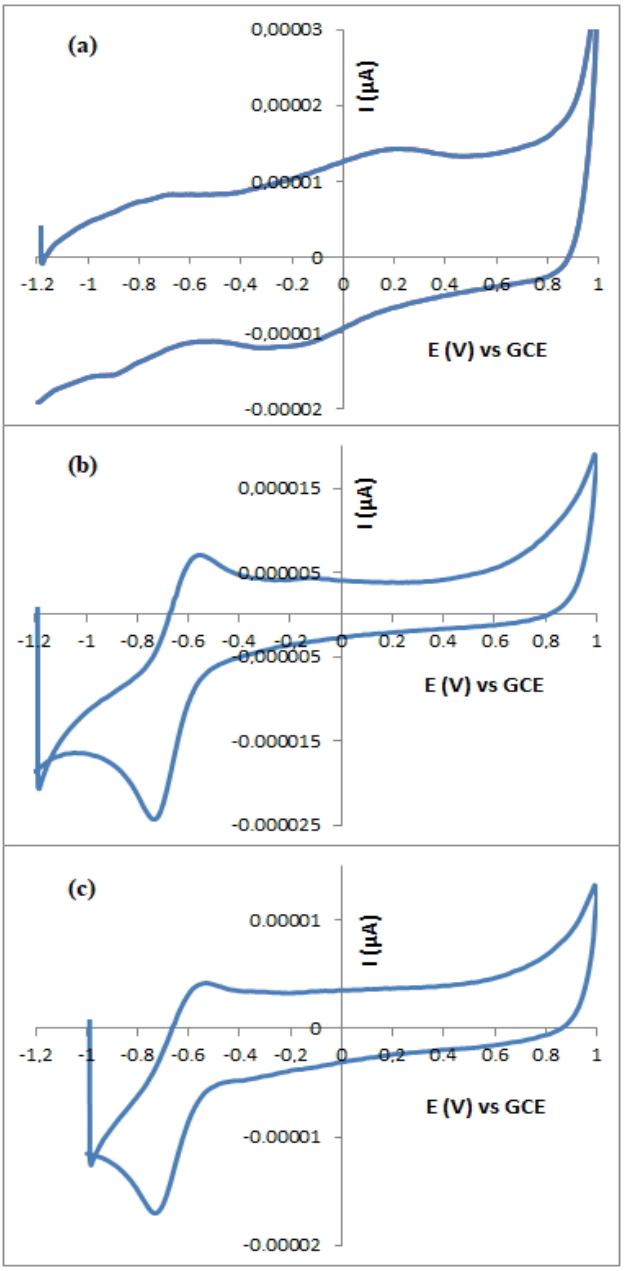

Figure 2. Cyclic voltammograms of (a) ZnPc, (b) Co(II)Pc and (c) Cd(II)Pc

Figure 3 (a) illustrates the in-situ UV–Visible spectral changes during the reduction process at a constant potential of -0.86 V, while Figure 3 (b) shows the spectral changes during the oxidation process at a constant potential of 0.20 V for **Pc-6**. In both Figure 3 (a) and (b), it can be observed that the entire absorption bands were reduced during reduction and oxidized during oxidation, without the formation of any new bands. This behavior suggests that the complex undergoes ring decomposition immediately after the redox process.

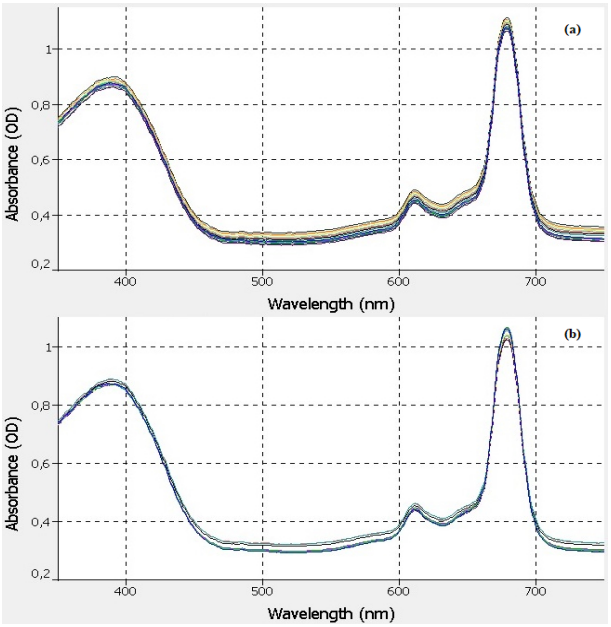

Figure 3. In-situ UV–Vis spectra of ZnPc (DMSO, 0.1 M $TBABF_4$) at (**a**) −0.86 V, (**b**) 0.20 V

Figure 4 illustrates the UV-Vis in-situ spectral changes for complexes **Pc-7** and **Pc-8**. Upon closer examination of Figure 4 (b), it becomes evident that **Pc-8** also undergoes ring decomposition immediately after the redox process at a potential of -0.64 V. In Figure 4 (a), isosbestic points are seen on 387 nm, 572 nm, and 687 nm for **Pc-7**. Furthermore, new bands at 483 nm and 704 nm are formed. Isosbestic points are well-known indicators of a transition from one state to another.

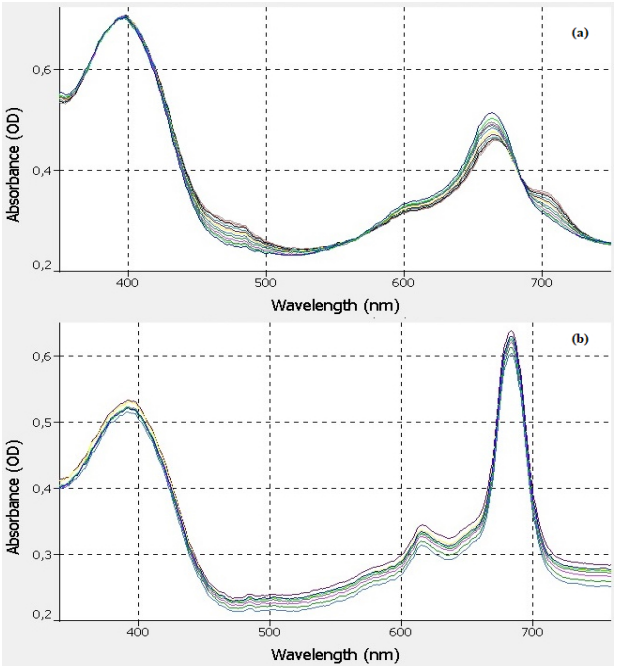

Figure 4. In-situ UV–Vis spectra (**a**) Co(II)Pc and (**b**) Cd(II)Pc (DMSO, 0.1 M $TBABF_4$) at potential of the (**a**)−0.65 V, (**b**)-0.64 V

The constant absorption spectrum observed at 684 nm in the Q band during constant electrolysis shows that no type of aggregation occurs. These spectral changes, along with the formation of clearly defined isosbestic points, suggest that they are due to ring-based reduction. Importantly, during any in-situ spectroelectrochemical process, the Q band remained unchanged. This behavior may result from the relative stabilization of the HOMO over the LUMO in MPc complexes [86]. However, in the specific case of Co(II)Pc (Pc-7), the nature of the newly formed bands requires a more detailed assignment. The appearance of a new absorption band in the visible region (around 450–480 nm) is often characteristic of a metal-centered reduction, leading to the formation of $[Co(I)Pc(-2)]^-$ species. This potential Co(I) formation represents one of the most original findings of the study, as it distinguishes the redox behavior of the cobalt complex from the ring-reduced products observed in the Zn(II) and Cd(II) derivatives.

3.4. Quantum Chemical Calculations

To better understand the reaction mechanism, it is crucial to examine the quantum chemical parameters such as HOMO, LUMO, and the band gap (ΔE) which reflects the energy difference between them. **Accordingly, the calculated electronic properties and energy levels of compound 5, obtained at the B3LYP/6-311++G(d,p) level of theory, are summarized and presented in Table 1.**

Table 1. The quantum chemical parameters of compound **5** (B3LYP 6.311++G(d,p) (eV))

	Compund 5
	B3LYP
E_{HOMO}	-7,02979
E_{LUMO}	-2,76196
Band Gap, ΔE	4,26784
Chemical hardness, η	2,13392
Global softness, σ	0,46862
Global electrophilicity, ω	5,61633
Ionization potential, I	7,02979
Electron affinity, A	2,76196
Electronegativity, χ	4,89587

Analysis of the HOMO and LUMO provides valuable insights into the specific regions of the molecule that are involved in the reaction. The electron-donating tendency is associated with the HOMO, indicating that molecules with higher HOMO energy levels are more prone to donate electrons readily. Conversely, the electron-accepting propensity is linked to the LUMO, suggesting that molecules with lower LUMO energy levels are more inclined to accept electrons easily. Therefore, molecules exhibiting higher HOMO levels and lower LUMO levels tend to display higher reactivity.

Chemical hardness, denoted as η, characterizes the resistance of the electron cloud to polarization. This factor is key in enabling ligands to interact with metal ions of similar hardness, thus influencing their reactivity. The global softness (σ) and chemical hardness are both explained in terms of the energy values of the HOMO and LUMO [33].

Chemical hardness,

$$\eta = \frac{E_{LUMO} - E_{HOMO}}{2} = \frac{I - A}{2} \quad (1)$$

Global softness,

$$\sigma = \frac{1}{\eta} \quad (2)$$

The chemical potential is expressed as the derivative of energy at equilibrium elative to the number of electrons, in a fixed molecular geometry, μ:

The chemical potential of a system,

$$\mu = \frac{E_{HOMO_0} + E_{LUMO}}{2} \quad (3)$$

The chemical potential is the negative of electronegativity, χ, while the global electrophilicity index (ω) is derived using Eq. (5).

Electronegativity,

$$\chi = \frac{I + A}{2} \quad (4)$$

The global electrophilicity index

$$\omega = \frac{\chi^2}{2\eta} \quad (5)$$

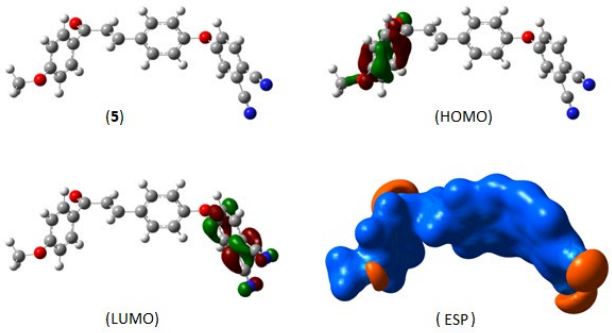

Figure 5. HOMO and LUMO orbitals, ESP and the optimized geometric structures of phthalonitrile **5**

Figure 5 illustrates the HOMO, LUMO, ESP and the optimized geometric structures of phthalonitrile **5**. The ESP map indicates which atom has a higher electron density on the surface

3.5. Catalytic Oxidation of 2-Mercaptoethanol

The oxidation of 2-mercaptoethanol is a commonly studied reaction for evaluating the catalytic performance of Co(II) phthalocyanine. In this investigation, **Pc-7**, Co(II)phthalocyanine plays a crucial role by acting as a bridge between the thiolate anion RS- and the oxygen (O_2) derived from the air. Co(II)phthalocyanine facilitates the connection between RS^- and O_2 through the central Co(II) atom at the core of the phthalocyanine. In the course of this coordination, an electron transfer reaction happens, with electrons migrating from the thiol group to oxygen through the central Co(II). As a result, thiol radicals are formed, which then combine to create disulfide compounds. Disulfide compounds are less reactive than thiol compounds, leading to a decrease in the reactivity of the thiol compounds due to this oxidation reaction. The overall reaction between 2-mercaptoethanol and oxygen, as shown in Equation (6), forms the basis for evaluating catalytic activity [33, 38,87]:

$$4R\text{-}S^- + O_2 \rightarrow R\text{-}S\text{-}S\text{-}R + 4OH^- \quad (6)$$

In this reaction, four molecules of thiolate ($R\text{-}S^-$) react with oxygen (O_2) to form a disulfide compound (R-S-S-R) and four hydroxide ions ($4OH^-$). In order to begin the reaction, NaOH is introduced into the thiol (RSH) solution, leading to proton loss and the formation of thiolate (RS^-). Co(II)Pc then will catalyze the oxidation of 2-mercaptoethanol. The progress of the oxidation

reaction and the catalytic efficiency of Pc-7 were confirmed by measuring the oxygen consumption, as depicted in Figure 6.

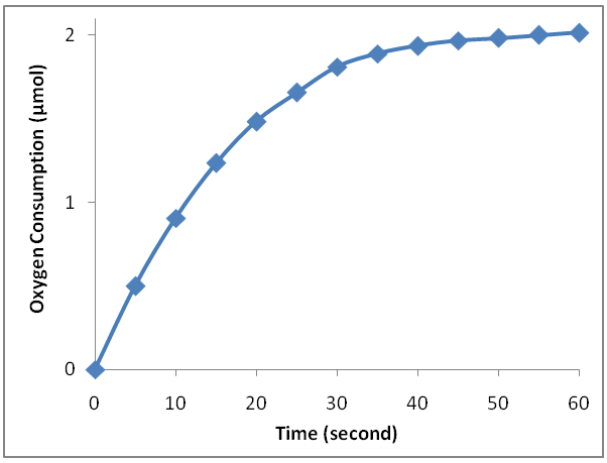

Figure 6. Oxygen consumption in the oxidation of 2-mercaptoethanol by **Pc-7**

The catalytic performance of the synthesized Co(II)Pc was numerically evaluated by comparing its TON value (45.84) with previously reported similar systems. For instance, in a study conducted by Karaca [87], cobalt (II) phthalocyanines bearing furan and thiophene chalcones exhibited TON values of 16.6 and 15.9, respectively, for the oxidation of 2-mercaptoethanol under similar conditions. The significantly higher TON value obtained in our study (45.84) suggests that the specific substitution pattern and the electronic nature of the chalcone groups on our complex effectively enhance the catalytic efficiency and stability of the cobalt center during the oxidation process.

4. Conclusion

In summary, this study successfully synthesized and characterized new Zn, Co(II), and Cd(II) phthalocyanines with chalcone groups attached to their periphery. The synthesis process began with the preparation of the chalcone group compound **3** in an ethanol-water mixture. Subsequently, this chalcone group was used to react with 4-nitrophthalonitrile through an SN_{Ar}-type substitution reaction. A well-established method for phthalocyanine synthesis was employed to directly synthesize all three phthalocyanines: ZnPc, Co(II)Pc and Cd(II)Pc.

The structural integrity of all synthesized compounds was confirmed using a range of techniques, including FT-IR, ^{1}H NMR, ^{13}C NMR, and MALDI-TOF MS. Cyclic voltammetry revealed one reduction and one oxidation reaction for ZnPc, one reduction reaction for Co(II)Pc, and one reduction reaction for Cd(II)Pc. Spectroelectrochemical investigations provided insights into the ring-based redox potentials for these metal phthalocyanines. ZnPc exhibited immediate complex decomposition following the ring-based redox potential, while Cd(II)Pc also displayed a ring-based decomposition.

Furthermore, Co(II)Pc was explored as a catalyst in the oxidation of 2-mercaptoethanol. This reaction, known for evaluating the catalytic activity of metallophthalocyanines, yielded significant results. The calculated parameters included a turnover number (TON) of 45.84, an initial reaction rate of 0.084 $\mu mol \cdot s^{-1}$, and oxygen consumption at a rate of 36.25 $\mu mol \cdot L^{-1} \cdot min^{-1}$ over time.

Article Information Form

Acknowledgments
This research is funded by Sakarya University Scientific Research Projects Unit (BAPK 2025-27-70-50).

Authors' Contribution
H. Karaca: Conceptualisation, Experimental Section, Writing, Computational Chemistry Calculations and Catalysis experiments and calculations.
Ö .Güven: Experimental Section and preparation of Figures.
M.Dinesh Kumar: Writing and Computational Calculations.
R. Ravikumar: Writing, Computational Chemistry Calculations

The Declaration of Conflict of Interest/ Common Interest
No conflict of interest or common interest has been declared by authors.

Artificial Intelligence Statement
No artificial intelligence tools were used while writing this article.

Copyright Statement
Authors own the copyright of their work published in the journal and their work is published under the CC BY-NC 4.0 license.

References

[1] G. Güney and S. Gördük, "Photophysical and photochemical studies on non-peripherally and peripherally Ga(III) chloro phthalocyanines in different solvents," *J. Organomet. Chem.*, vol. 999, Art. no. 122813, 2023, doi: 10.1016/j.jorganchem.2023.122813.

[2] L. Hu, H. Han, Z. Xu, K. Song, and F. Wang, "Synthesis, photophysical, and photochemical properties of functional molecules based on a novel zinc(II) phthalocyanine-1,8-naphthalimide skeleton," *J. Mol. Struct.*, vol. 1291, Art. no. 136007, 2023, doi: 10.1016/j.molstruc.2023.136007.

[3] R. Zugle, C. Litwinski, and T. Nyokong, "Photophysical characterization of dysprosium, erbium and lutetium phthalocyanines tetrasubstituted with phenoxy groups at non-peripheral positions," *Polyhedron*, vol. 30, no. 9, pp. 1612–1619, 2011, doi: 10.1016/j.poly.2011.03.030.

[4] A. M. Sevim, C. Ilgün, and A. Gül, "Preparation of heterogeneous phthalocyanine catalysts by cotton fabric dyeing," *Dyes Pigments*, vol. 89, no. 2, pp. 162–168, 2011, doi: 10.1016/j.dyepig.2010.10.008.

[5] E. Güzel *et al.*, "Zinc and chloroindium complexes of furan-2-ylmethoxy substituted phthalocyanines: Preparation and investigation of aggregation, singlet oxygen generation, antioxidant and antimicrobial properties," *Synth. Met.*, vol. 245, pp. 127–134, 2018, doi: 10.1016/j.synthmet.2018.08.018.

[6] A. Günsel, E. Güzel, A. T. Bilgiçli, İ. Şişman, and M. N. Yaraşır, "Synthesis of non-peripheral thioanisole-substituted phthalocyanines: Photophysical, electrochemical, photovoltaic, and sensing properties," *J. Photochem. Photobiol. A Chem.*, vol. 348, pp. 57–67, 2017, doi: 10.1016/j.jphotochem.2017.07.040.

[7] D. G. Solğun and M. S. Ağırtaş, "Synthesis of novel an axially substituted silicon phthalocyanine and determination of its selectivity for Fe^{3+}," *J. Mol. Struct.*, vol. 1286, Art. no. 135577, 2023, doi: 10.1016/j.molstruc.2023.135577.

[8] M. S. Ağırtaş, D. G. Solğun, B. Savaş, and T. Öztürk, "Synthesis and sensor properties of silicon phthalocyanine axially substituted with bis(prop-2-ynyloxy) groups and polymeric phthalocyanines bearing PEG substituent by 'click' chemistry," *Polycycl. Aromat. Compd.*, vol. 43, no. 4, pp. 3278–3290, 2023, doi: 10.1080/10406638.2022.2067195.

[9] H. Karaca, M. Teker, and A. Gül, "Catalytic oxidation of 2-mercaptoethanol by a water-soluble porhphyrazinatocobalt(II) complex," *Chem. J.*, vol. 6, no. 1, pp. 55–58, 2016.

[10] H. Karaca, N. Akçay, and M. Teker, "Porphyrazine immobilization on polyester fabric and heterogeneous catalytic application on oxidation of 2-mercaptoethanol," *Fresenius Environ. Bull.*, vol. 25, no. 5, pp. 1714–1718, 2016.

[11] J. P. Mensing, A. Wisitsoraat, A. Tuantranont, and T. Kerdcharoen, "Inkjet-printed sol–gel films containing metal phthalocyanines/porphyrins for opto-electronic nose applications," *Sens. Actuators B Chem.*, vol. 176, pp. 428–436, 2013, doi: 10.1016/j.snb.2012.09.053.

[12] M. Gay-Martín, E. Díez-Arévalo, M. L. Rodríguez-Méndez, and J. A. de Saja Sáez, "Electrochemical quartz crystal microbalance analysis of the oxidation

reaction of phenols found in wines at lutetium bisphthalocyanine electrodes," *Sens. Actuators B Chem.*, vol. 185, pp. 24–31, 2013, doi: 10.1016/j.snb.2013.04.115.

[13] K. B. Manjunatha, R. Dileep, G. Umesh, and B. R. Bhat, "Nonlinear optical and all-optical switching studies of novel ruthenium complex," *Opt. Laser Technol.*, vol. 52, pp. 103–108, 2013, doi: 10.1016/j.optlastec.2013.04.019.

[14] S. Gördük, O. Avcıata, and U. Avcıata, "Photocatalytic degradation of methylene blue under visible light irradiation by non-peripherally tetra-substituted phthalocyanine–TiO_2 nanocomposites," *Inorg. Chim. Acta*, vol. 471, pp. 137–147, 2018, doi: 10.1016/j.ica.2017.11.004.

[15] L. Grządziel and M. Krzywiecki, "Quantitative correlation between air-induced changes of electronic parameters and morphological features of copper phthalocyanine thin-film surfaces," *Mater. Chem. Phys.*, vols. 149–150, pp. 574–581, 2015, doi: 10.1016/j.matchemphys.2014.11.008.

[16] G. K. Kantar, N. Baltaş, E. Menteşe, and S. Şaşmaz, "Microwave-assisted synthesis and investigation of xanthine oxidase inhibition of new phthalonitrile and phthalocyanines containing morpholino-substituted 1,2,4-triazole-3-one," *J. Organomet. Chem.*, vol. 787, pp. 8–13, 2015, doi: 10.1016/j.jorganchem.2015.03.033.

[17] R. A. Shoukat Ali *et al.*, "DC electrical conductivity studies of tetra 2-(furan-2-yl)-1,3,4-oxadiazole substituted metal(II) phthalocyanines," *Mater. Today Proc.*, vol. 49, pt. 3, pp. 644–649, 2022, doi: 10.1016/j.matpr.2021.05.163.

[18] A. Kumar, R. Meunier-Prest, F. Herbst, O. Heintz, E. Lesniewska, and M. Bouvet, "Covalent grafting of aryls to modulate the electrical properties of phthalocyanine-based heterostructures: Application to ammonia sensing," *Chem. Eng. J.*, vol. 436, Art. no. 135207, 2022, doi: 10.1016/j.cej.2022.135207.

[19] A. Kumar, G. Zhang, W. Liu, and X. Sun, "Electrocatalysis and activity descriptors with metal phthalocyanines for energy conversion reactions," *J. Electroanal. Chem.*, vol. 922, Art. no. 116799, 2022, doi: 10.1016/j.jelechem.2022.116799.

[20] S. Abdel Aal and D. Awadh, "The effect of anchoring group on the performances of metal-free phthalocyanine and metallophthalocyanine dye/titanium dioxide interface for dye-sensitized solar cells," *Surf. Interfaces*, vol. 32, Art. no. 102089, 2022, doi: 10.1016/j.surfin.2022.102089.

[21] H. Sarıoğulları, I. F. Şengül, and A. G. Gürek, "Comparative study on sensing and optical properties of carbazole-linked novel zinc(II) and cobalt(II) phthalocyanines," *Polyhedron*, vol. 227, Art. no. 116139, 2022, doi: 10.1016/j.poly.2022.116139.

[22] S. Zhang *et al.*, "Interface engineering via phthalocyanine decoration of perovskite solar cells with high efficiency and stability," *J. Power Sources*, vol. 438, Art. no. 226987, 2019, doi: 10.1016/j.jpowsour.2019.226987.

[23] M. Chaabene, B. Gassoumi, P. Mignon, R. Ben Chaâbane, and A. R. Allouche, "New zinc phthalocyanine derivatives for nitrogen dioxide sensors: A theoretical optoelectronic investigation," *J. Mol. Graph. Model.*, vol. 88, pp. 174–182, 2019, doi: 10.1016/j.jmgm.2019.01.008.

[24] A. L. Uğur, A. Erdoğmuş, A. Koca, and U. Avcıata, "Synthesis, spectroscopic, electrochemical and spectroelectrochemical properties of metal-free, manganese, and cobalt phthalocyanines bearing peripherally

octakis[4-(thiophen-3-yl)phenoxy] substituents," *Polyhedron*, vol. 29, no. 18, pp. 3310–3317, 2010, doi: 101016/j.poly.2010.09.008.

[25] A. A. Ensafi and H. Karimi-Maleh, "Modified multiwall carbon nanotubes paste electrode as a sensor for simultaneous determination of 6-thioguanine and folic acid using ferrocenedicarboxylic acid as a mediator," *J. Electroanal. Chem.*, vol. 640, nos. 1–2, pp. 75–83, 2010, doi: 10.1016/j.jelechem.2010.01.010.

[26] H. N. Raval, D. S. Sutar, and V. R. Rao, "Copper(II) phthalocyanine-based organic electronic devices for ionizing radiation dosimetry applications," *Org. Electron.*, vol. 14, no. 5, pp. 1281–1290, 2013, doi: 10.1016/j.orgel.2013.02.026.

[27] H. Mizuseki, N. Igarashi, R. V. Belosludov, A. A. Farajian, and Y. Kawazoe, "Theoretical study of phthalocyanine–fullerene complex for a high-efficiency photovoltaic device using ab initio electronic structure calculation," *Synth. Met.*, vol. 138, nos. 1–2, pp. 281–283, 2003, doi: 10.1016/S0379-6779(02)01289-4.

[28] Z. Şahin, R. Meunier-Prest, F. Dumoulin, A. Kumar, Ü. İşci, and M. Bouvet, "Tuning of organic heterojunction conductivity by the substituents' electronic effects in phthalocyanines for ambipolar gas sensors," *Sens. Actuators B Chem.*, vol. 332, Art. no. 129505, 2021, doi: 10.1016/j.snb.2021.129505.

[29] E. Yabaş, E. Biçer, and A. Altındal, "Novel reduced graphene oxide/zinc phthalocyanine and reduced graphene oxide/cobalt phthalocyanine hybrids as high-sensitivity room-temperature volatile organic compound gas sensors," *J. Mol. Struct.*, vol. 1271, Art. no. 134076, 2023, doi: 10.1016/j.molstruc.2022.134076.

*[30] S. Gai, B. Wang, X. Wang, R. Zhang, S. Miao, and Y. Wu, "Ultrafast NH_3 gas sensor based on phthalocyanine-optimized non-covalent hybrid of carbon nanotubes with pyrrole," *Sens. Actuators B Chem.*, vol. 357, Art. no. 131352, 2022, doi: 10.1016/j.snb.2021.131352.

[31] T. Miyata, S. Kawaguchi, M. Ishii, and T. Minami, "High-sensitivity chlorine gas sensors using Cu–phthalocyanine thin films," *Thin Solid Films*, vol. 425, nos. 1–2, pp. 255–259, 2003, doi: 10.1016/S0040-6090(02)01129-X.

[32] A. K. Sharma, A. K. Debnath, D. K. Aswal, and A. Mahajan, "Room-temperature ppb-level detection of chlorine using peripherally alkoxy-substituted phthalocyanine/SWCNTs-based chemiresistive sensors," *Sens. Actuators B Chem.*, vol. 350, Art. no. 130870, 2022, doi: 10.1016/j.snb.2021.130870.

[33] H. Karaca *et al.*, "Metallophthalocyanines derived with phenyl sulfide by bridging triazole using click chemistry: Synthesis, computational study, redox chemistry and catalytic activity," *J. Mol. Struct.*, vol. 1236, Art. no. 130225, 2021, doi: 10.1016/j.molstruc.2021.130225.

[34] G. G. Çelik *et al.*, "Influence of spacer and donor groups as tetraphenylethylene or triphenylamine in asymmetric zinc phthalocyanine dyes for dye-sensitized solar cells," *J. Photochem. Photobiol. A Chem.*, vol. 444, Art. no. 114962, 2023, doi: 10.1016/j.jphotochem.2023.114962.

[35] G. G. Köse, G. K. Karaoğlan, Y. E. Maden, and A. Koca, "Influence of 2-naphthoic acid anchoring groups on the photovoltaic performance of zinc phthalocyanine-based photosensitizers in dye-sensitized solar cells," *J. Electroanal. Chem.*, vol. 945, Art. no. 117691, 2023, doi: 10.1016/j.jelechem.2023.117691.

[36] A. C. Yüzer *et al.*, "Solution-processed small-molecule organic solar cells based on non-aggregated zinc phthalocyanine derivatives: A comparative experimental and theoretical study," *Mater. Sci. Semicond. Process.*, vol. 129, Art. no. 105777, 2021, doi: 10.1016/j.mssp.2021.105777.

[37] H. Karaca, B. Çayeğil, and S. Sezer, "Synthesis, characterization and metal-sensing applications of novel chalcone-substituted phthalocyanines," *Synth. Met.*, vol. 215, pp. 134–141, 2016, doi: 10.1016/j.synthmet.2016.02.007.

[38] H. Karaca, "Redox chemistry, spectroelectrochemistry and catalytic activity of novel synthesized phthalocyanines bearing four Schiff bases on the periphery," *J. Organomet. Chem.*, vol. 822, pp. 39–45, 2016, doi: 10.1016/j.jorganchem.2016.08.013.

[39] H. Karaca, S. Sezer, and C. Tanyeli, "Synthesis of L-prolinol-substituted novel optically active phthalocyanines," *Dyes Pigments*, vol. 90, no. 2, pp. 100–105, 2011, doi: 10.1016/j.dyepig.2010.12.003.

[40] M. Kınalı *et al.*, "Chalcone-based dipolar cycloaddition of novel heteroaromatic compounds: Their anticancer examination," *J. Mol. Struct.*, vol. 1293, Art. no. 136244, 2023, doi: 10.1016/j.molstruc.2023.136244.

[41] H. V. Chavan, S. D. Ganapure, N. N. Mali, and P. S. Bhale, "Synthesis, characterization and biological evaluation of N-substituted indolyl chalcones as anticancer, anti-inflammatory and antioxidant agents," *Mater. Today Proc.*, vol. 73, pt. 3, pp. 396–402, 2023, doi: 10.1016/j.matpr.2022.09.264.

[42] I. F. de Farias *et al.*, "Synthesis, characterization and molecular docking study of pyrazolines synthesized from chalcones: Antioxidant and acetylcholinesterase activities," *J. Mol. Struct.*, vol. 1291, Art. no. 135961, 2023, doi: 10.1016/j.molstruc.2023.135961.

[43] A. Suyambulingam, S. Nair, and K. Chellapandian, "Synthesis, spectral characterization of novel chalcones based oxazines derivatives and screening of their antimicrobial and antioxidant activity," *J. Mol. Struct.*, vol. 1268, Art. no. 133708, 2022, doi: 10.1016/j.molstruc.2022.133708.

[44] A. Siddiqa *et al.*, "Synthesis, molecular docking, bio-evaluation and quantitative structure activity relationship of new chalcone derivatives as antioxidants," *J. Mol. Struct.*, vol. 1277, Art. no. 134814, 2023, doi: 10.1016/j.molstruc.2022.134814.

[45] M. Yadav, K. Lal, A. Kumar, P. Singh, V. K. Vishvakarma, and R. Chandra, "Click reaction inspired synthesis, antimicrobial evaluation and in silico docking of some pyrrole-chalcone linked 1,2,3-triazole hybrids," *J. Mol. Struct.*, vol. 1273, Art. no. 134321, 2023, doi: 10.1016/j.molstruc.2022.134321.

[46] J. Moreira *et al.*, "New diarylpentanoids and chalcones as potential antimicrobial adjuvants," *Bioorg. Med. Chem. Lett.*, vol. 67, Art. no. 128743, 2022, doi: 10.1016/j.bmcl.2022.128743.

[47] T. N. M. Musthafa, K. Snigdha, A. M. Asiri, T. R. Sobahi, and M. Asad, "Green synthesis of chromonyl chalcone and pyrazoline as potential antimicrobial agents—DFT, molecular docking and antimicrobial studies," *J. Mol. Struct.*, vol. 1271, Art. no. 133993, 2023, doi: 10.1016/j.molstruc.2022.133993.

[48] S. Burmaoglu, E. A. Kazancioglu, M. Z. Kazancioglu, M. A. Alagoz, A. Dogen, and O. Algul, "Synthesis, in vitro biological evaluation, and molecular docking studies of novel biphenyl chalcone derivatives as

antimicrobial agents," *Polycycl. Aromat. Compd.*, vol. 42, no. 9, pp. 5948–5961, 2022, doi: 10.1080/10406638.2021.1962925.

[49] D. Ušjak, B. Ivković, D. D. Božić, L. Bošković, and M. Milenković, "Antimicrobial activity of novel chalcones and modulation of virulence factors in hospital strains of *Acinetobacter baumannii* and *Pseudomonas aeruginosa*," *Microb. Pathog.*, vol. 131, pp. 186–196, 2019, doi: 10.1016/j.micpath.2019.04.015.

[50] X. Xu *et al.*, "Synthesis, in vitro cytotoxicity evaluation and mechanism of 5′-monosubstituted chalcone derivatives as antitumor agents," *Bioorg. Med. Chem. Lett.*, vol. 85, Art. no. 129239, 2023, doi: 10.1016/j.bmcl.2023.129239.

[51] M. M. Amin *et al.*, "Design, synthesis, cytotoxic activities, and molecular docking of chalcone hybrids bearing 8-hydroxyquinoline moiety with dual tubulin/EGFR kinase inhibition," *Bioorg. Chem.*, vol. 134, Art. no. 106444, 2023, doi: 10.1016/j.bioorg.2023.106444.

[52] A. Beytur *et al.*, "Hexa-substituted cyclotriphosphazene derivatives containing hetero-ring chalcones: Synthesis, in vitro cytotoxic activity and their DNA damage determination," *Bioorg. Chem.*, vol. 127, Art. no. 105997, 2022, doi: 10.1016/j.bioorg.2022.105997.

[53] S. Koldas, I. Demirtas, D. Mutlu, M. N. Atalar, H. Ünver, and Ş. Arslan, "New cytotoxic chalcone derivatives from *Astragalus ponticus* Pall.," *Nat. Prod. Res.*, vol. 36, no. 18, pp. 4672–4680, 2022, doi: 10.1080/14786419.2021.2012771.

[54] L. Devi, G. Sharma, R. Kant, S. K. Shukla, and N. Rastogi, "Regioselective synthesis of functionalized pyrazole-chalcones via a base-mediated reaction of diazo compounds with pyrylium salts," *Org. Biomol. Chem.*, vol. 19, no. 18, pp. 4132–4136, 2021, doi: 10.1039/D1OB00274K.

[55] S. Farooq and Z. Ngaini, "One-pot and two-pot methods for chalcone-derived pyrimidines synthesis and applications," *J. Heterocycl. Chem.*, vol. 58, no. 6, pp. 1209–1224, 2021, doi: 10.1002/jhet.4226.

[56] N. Deshmukh and A. Shinde, "An efficient, ultrasound-induced ring closure of hydroxy chalcone in 2-ethoxy ethanol as an green reaction medium and study of antimicrobial potential," *Chem. Data Collect.*, vol. 31, Art. no. 100606, 2021, doi: 10.1016/j.cdc.2020.100606.

[57] C. F. S. Guazelli *et al.*, "Antioxidant and anti-inflammatory effects of hesperidin methyl chalcone in experimental ulcerative colitis," *Chem.-Biol. Interact.*, vol. 333, Art. no. 109315, 2021, doi: 10.1016/j.cbi.2020.109315.

[58] S. C. Carr, M. A. Torres, J. S. Morris, P. J. Facchini, and K. K. S. Ng, "Structural studies of codeinone reductase reveal novel insights into aldo-keto reductase function in benzylisoquinoline alkaloid biosynthesis," *J. Biol. Chem.*, vol. 297, no. 4, Art. no. 101211, 2021, doi: 10.1016/j.jbc.2021.101211.

[59] H. L. Qin, Z. W. Zhang, L. Ravindar, and K. P. Rakesh, "Antibacterial activities with the structure–activity relationship of coumarin derivatives," *Eur. J. Med. Chem.*, vol. 207, Art. no. 112832, 2020, doi: 10.1016/j.ejmech.2020.112832.

[60] D. Das, "Lemon juice-mediated efficient and eco-friendly organic transformations," *Tetrahedron Lett.*, vol. 61, no. 36, Art. no. 152298, 2020, doi: 10.1016/j.tetlet.2020.152298.

[61] K. Trush and P. Paľove-Balang, "Biosynthesis and role of isoflavonoids in legumes under different environmental conditions," *Plant Stress*, vol. 8, Art. no.

100153, Jun. 2023, doi: 10.1016/j.stress.2023.100153.

[62] J. Ma, J. Zhang, and Z. Shen, "Two unusual isoflavonoids from *Campylotropis hirtella*—A new biosynthesis route of flavonoids," *Tetrahedron Lett.*, vol. 58, no. 15, pp. 1462–1466, 2017, doi: 10.1016/j.tetlet.2017.02.080.

[63] A. Murugesan, R. M. Gengan, R. Rajamanikandan, M. Ilanchelian, and C.-H. Lin, "One-pot synthesis of Claisen–Schmidt reaction through (E)-chalcone derivatives: Spectral studies in human serum albumin protein binding and molecular docking investigation," *Synth. Commun.*, vol. 47, no. 20, pp. 1884–1904, 2017, doi: 10.1080/00397911.2017.1355466.

[64] A. Murugesan, R. M. Gengan, and C.-H. Lin, "Efficient synthesis of ethyl-piperazinyl quinolinyl-(E)-chalcone derivatives via Claisen–Schmidt reaction by using TiO_2-BPTETSA catalyst," *J. Taiwan Inst. Chem. Eng.*, vol. 80, pp. 852–866, 2017, doi: 10.1016/j.jtice.2017.07.014.

[65] M. N. Arshad *et al.*, "Synthesis, crystal structures, spectroscopic and nonlinear optical properties of chalcone derivatives: A combined experimental and theoretical study," *J. Mol. Struct.*, vol. 1141, pp. 142–156, 2017, doi: 10.1016/j.molstruc.2017.03.090.

[66] D. Ergüntürk, M. B. Gürdere, Y. Budak, and M. Ceylan, "Synthesis, characterization, and investigations of antimicrobial activity of 6,6-dimethyl-3-aryl-3′,4′,6,7-tetrahydro-1′H,3H-spiro[benzofuran-2,2′-naphthalene]-1′,4(5H)-dione," *Synth. Commun.*, vol. 47, no. 16, pp. 1501–1506, 2017, doi: 10.1080/00397911.2017.1334918.

[67] N. Ndebele and T. Nyokong, "Electrocatalytic behaviour of chalcone-substituted Co, Cu, Mn and Ni phthalocyanines towards the detection of nitrite," *J. Electroanal. Chem.*, vol. 926, Art. no. 116951, Dec. 2022, doi: 10.1016/j.jelechem.2022.116951.

[68] G. Sarkı, H. Kantekin, H. Yalazan, N. Kahriman, Z. Bıyıklıoğlu, and V. Serdaroğlu, "Synthesis, characterization and electrochemical studies of metal-free and metallophthalocyanines containing two different chalcone units substituted on peripheral positions," *J. Mol. Struct.*, vol. 1196, pp. 592–603, 2019, doi: 10.1016/j.molstruc.2019.05.123.

[69] Y. I. Openda, B. Babu, and T. Nyokong, "Novel cationic-chalcone phthalocyanines for photodynamic therapy eradication of *S. aureus* and *E. coli* bacterial biofilms and MCF-7 breast cancer," *Photodiagn. Photodyn. Ther.*, vol. 38, Art. no. 102863, Jun. 2022, doi: 10.1016/j.pdpdt.2022.102863.

[70] T. Arslan, "Design and synthesis of novel peripherally tetra-chalcone-substituted phthalocyanines and their inhibitory effects on acetylcholinesterase and carbonic anhydrases (hCA I and II)," *J. Organomet. Chem.*, vol. 951, Art. no. 122021, 2021, doi: 10.1016/j.jorganchem.2021.122021.

[71] X. F. Zhang, Y. Lin, W. Guo, and J. Zhu, "Spectroscopic insights on imidazole-substituted phthalocyanine photosensitizers: Fluorescence properties, triplet state and singlet oxygen generation," *Spectrochim. Acta A Mol. Biomol. Spectrosc.*, vol. 133, pp. 752–758, 2014, doi: 10.1016/j.saa.2014.06.063.

[72] H. Karaca and S. Kazancı, "The metal sensing applications of chalcones: The synthesis, characterization and theoretical calculations," *J. Mol. Struct.*, vol. 1248, Art. no. 131454, Jan. 2022, doi: 10.1016/j.molstruc.2021.131454.

[73] A. Baran, S. Çol, E. Karakılıç, and F. Özen, "Photophysical, photochemical and DNA binding studies of prepared phthalocyanines," *Polyhedron*, vol. 175, Art. no. 114205, 2020, doi: 10.1016/j.poly.2019.114205.

[74] H. Shinohara, O. Tsaryova, G. Schnurpfeil, and D. Wöhrle, "Differently substituted phthalocyanines: Comparison of calculated energy levels, singlet oxygen quantum yields, photo-oxidative stabilities, photocatalytic and catalytic activities," *J. Photochem. Photobiol. A Chem.*, vol. 184, no. 1, pp. 50–57, 2006, doi: 10.1016/j.jphotochem.2006.03.024.

[75] Y. Pan, W. Chen, S. Lu, and Y. Zhang, "Novel aqueous-soluble cobalt phthalocyanine: Synthesis and catalytic activity on oxidation of 2-mercaptoethanol," *Dyes Pigments*, vol. 66, no. 2, pp. 115–121, 2005, doi: 10.1016/j.dyepig.2004.09.018.

[76] V. I. Iliev, A. I. Ileva, and L. D. Dimitrov, "Catalytic oxidation of 2-mercaptoethanol by cobalt(II)-phthalocyanine complexes intercalated in layered double hydroxides," *Appl. Catal. A Gen.*, vol. 126, no. 2, pp. 333–340, 1995, doi: 10.1016/0926-860X(95)00027-5.

[77] W. Chidawanyika and T. Nyokong, "Spectroscopic and photophysicochemical behaviour of novel cadmium phthalocyanine derivatives tetra-substituted at the alpha and beta positions," *J. Photochem. Photobiol. A Chem.*, vol. 202, nos. 2–3, pp. 99–106, 2009, doi: 10.1016/j.jphotochem.2008.11.014.

[78] M. J. Frisch *et al.*, *Gaussian 16*, Revision C.01. Wallingford, CT, USA: Gaussian, Inc., 2016.

[79] R. Dennington, T. A. Keith, and J. M. Millam, *GaussView*, ver. 6. Shawnee Mission, KS, USA: Semichem Inc., 2016.

[80] C. Lee, W. Yang, and R. G. Parr, "Development of the Colle–Salvetti correlation-energy formula into a functional of the electron density," *Phys. Rev. B*, vol. 37, no. 2, pp. 785–789, Jan. 1988, doi: 10.1103/PhysRevB.37.785.

[81] M. S. Ağırtaş, C. Karataş, and S. Özdemir, "Synthesis of some metallophthalocyanines with dimethyl 5-(phenoxy)-isophthalate substituents and evaluation of their antioxidant-antibacterial activities," *Spectrochim. Acta A Mol. Biomol. Spectrosc.*, vol. 135, pp. 20–24, 2015, doi: 10.1016/j.saa.2014.06.139.

[82] M. S. Ağırtaş and M. S. İzgi, "Synthesis and characterization of new metallophthalocyanines with four phenoxyacetamide units," *J. Mol. Struct.*, vol. 927, nos. 1–3, pp. 126–128, 2009, doi: 10.1016/j.molstruc.2009.03.011.

[83] M. S. Ağırtaş, "Highly soluble phthalocyanines with hexadeca-tert-butyl substituents," *Dyes Pigments*, vol. 79, no. 3, pp. 247–251, 2008, doi: 10.1016/j.dyepig.2008.03.004.

[84] M. S. Ağırtaş, "Non-aggregating phthalocyanines with bulky 2,4-di-tert-butylphenoxy substituents," *Dyes Pigments*, vol. 74, no. 2, pp. 490–493, 2007, doi: 10.1016/j.dyepig.2006.03.009.

[85] P. R. Somani and S. Radhakrishnan, "Electrochromic materials and devices: Present and future," *Mater. Chem. Phys.*, vol. 77, no. 1, pp. 117–133, Jan. 2003, doi: 10.1016/S0254-0584(01)00575-2.

[86] N. Nombona and T. Nyokong, "The synthesis, cyclic voltammetry and spectroelectrochemical studies of Co(II) phthalocyanines tetra-substituted at the α and β positions with phenylthio groups," *Dyes Pigments*, vol. 80, no. 1, pp. 130–135, 2009, doi: 10.1016/j.dyepig.2008.06.002.

[87] H. Karaca, “Catalytic oxidation of 2-mercaptoethanol by cobalt(II) phthalocyanines bearing chalcone with furan and thiophene,” *Sakarya Univ. J. Sci.*, vol. 22, no. 6, pp. 1699–1703, Dec. 2018, doi: 10.16984/saufenbilder.407781.